Supporting Information

for

From Twofold Completive to Integrative Self-sorting: a Five-Component Supramolecular Trapezoid

*Kingsuk Mahata, Michael Schmittel**

Center of Micro and Nanochemistry and Engineering, Organische Chemie I, Universität Siegen, Adolf-Reichwein-Str. 2, D-57068 Siegen, Germany,
*E-mail: **schmittel@chemie.uni-siegen.de***
Fax: (+49) 271-740-3270

Table of Contents

1	^{1}H and ^{13}C spectra	S2
2	ESI-MS spectra	S10
3	DPV	S16
4	Deconvolution of the DPV	S17

NMR Spectra

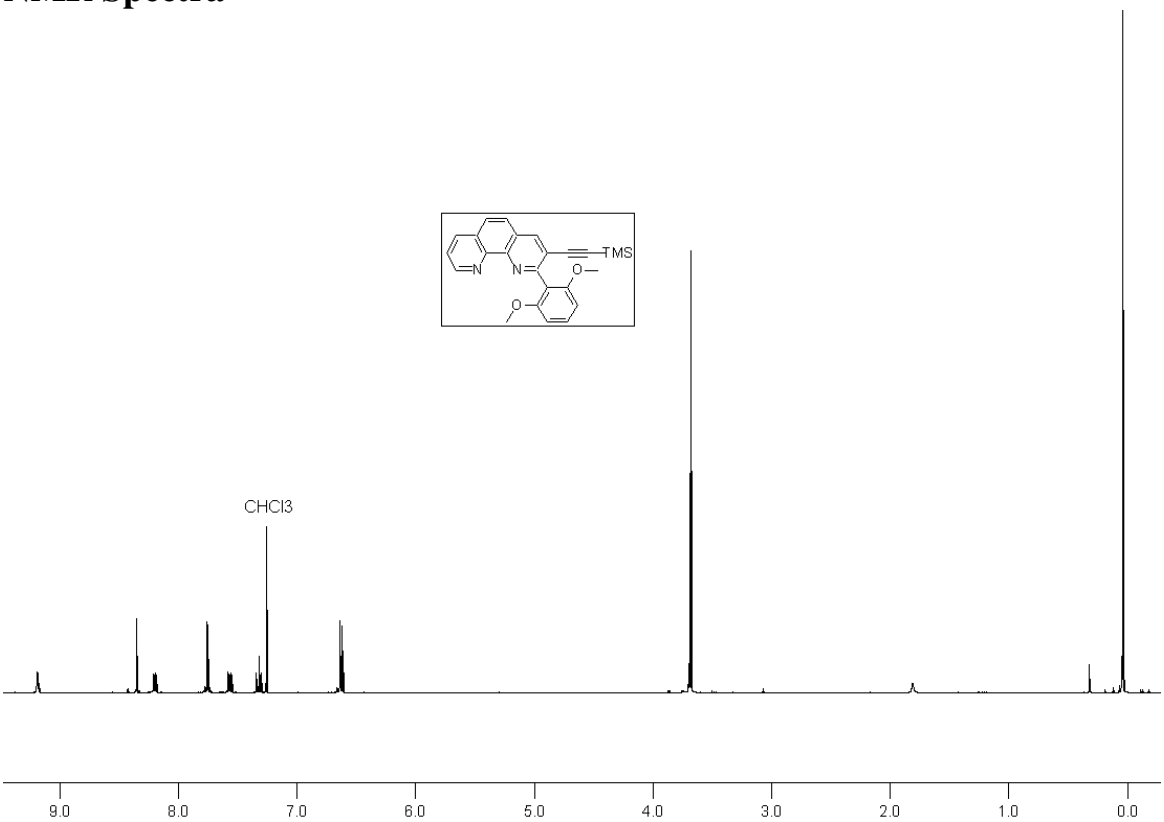

Figure S1. ^{1}H NMR spectrum (400 MHz, $CDCl_3$, 298 K) of 2-(2,6-dimethoxyphenyl)-3-trimethylsilanylethynyl-[1,10]phenanthroline (**9**).

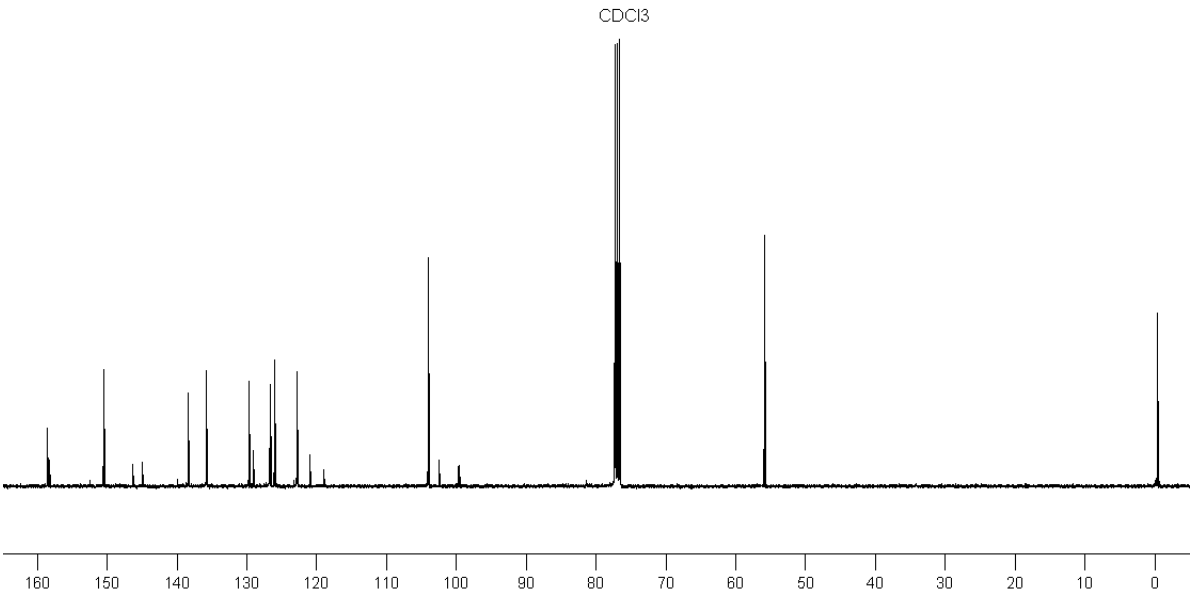

Figure S2. ^{13}C NMR spectrum (100 MHz, $CDCl_3$, 298 K) of 2-(2,6-dimethoxyphenyl)-3-trimethylsilanylethynyl-[1,10]phenanthroline (**9**).

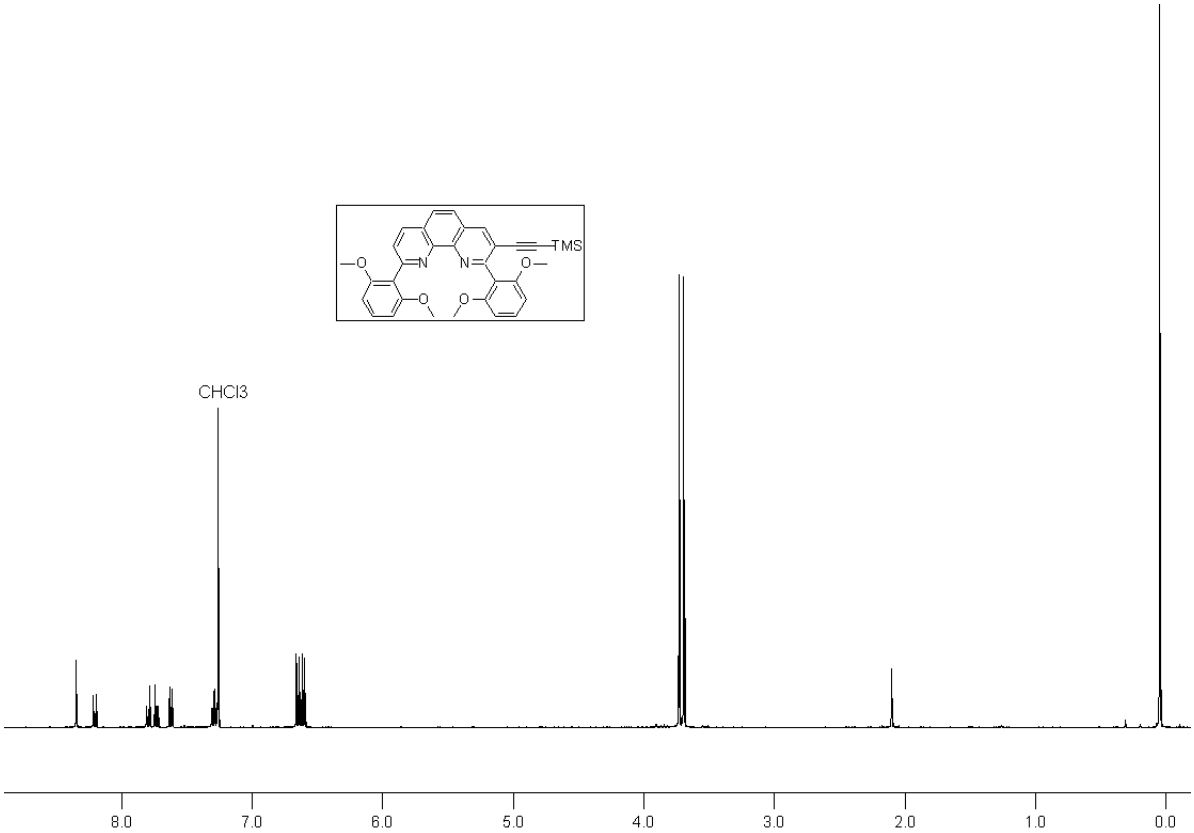

Figure S3. ^{1}H NMR spectrum (400 MHz, $CDCl_3$, 298 K) of 2,9-bis-(2,6-dimethoxyphenyl)-3-trimethylsilanylethynyl-[1,10]phenanthroline (**10**).

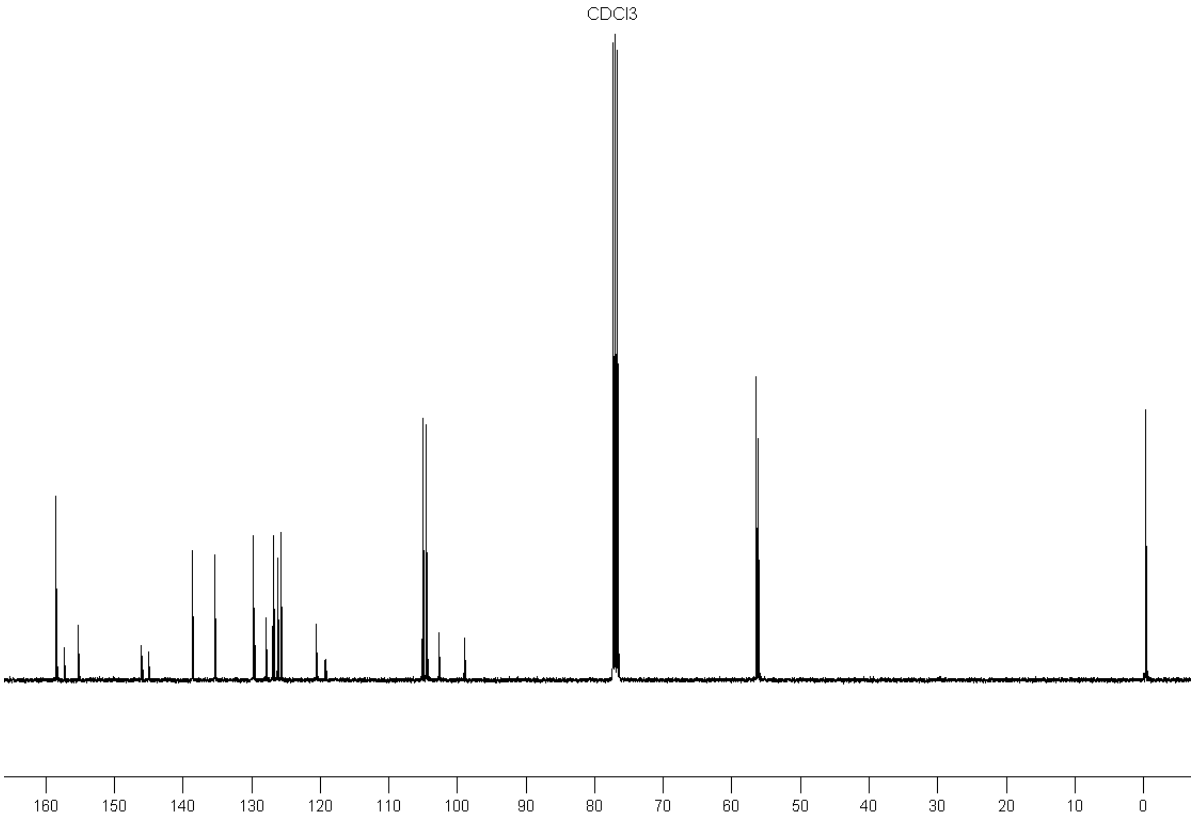

Figure S4. ^{13}C NMR spectrum (100 MHz, $CDCl_3$, 298 K) of 2,9-bis-(2,6-dimethoxyphenyl)-3-trimethylsilanylethynyl-[1,10]phenanthroline (**10**).

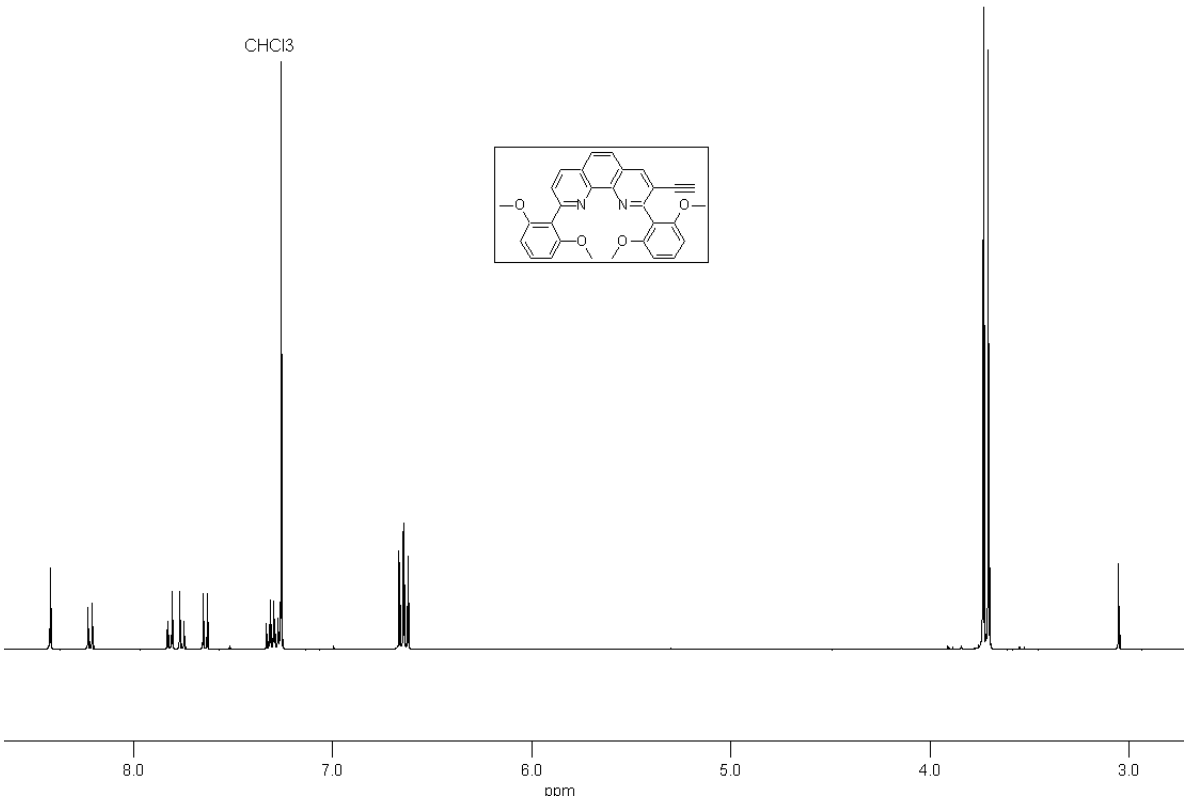

Figure S5. ^{1}H NMR spectrum (400 MHz, $CDCl_3$, 298 K) of 2,9-bis-(2,6-dimethoxyphenyl)-3-ethynyl-[1,10]-phenanthroline (**11**).

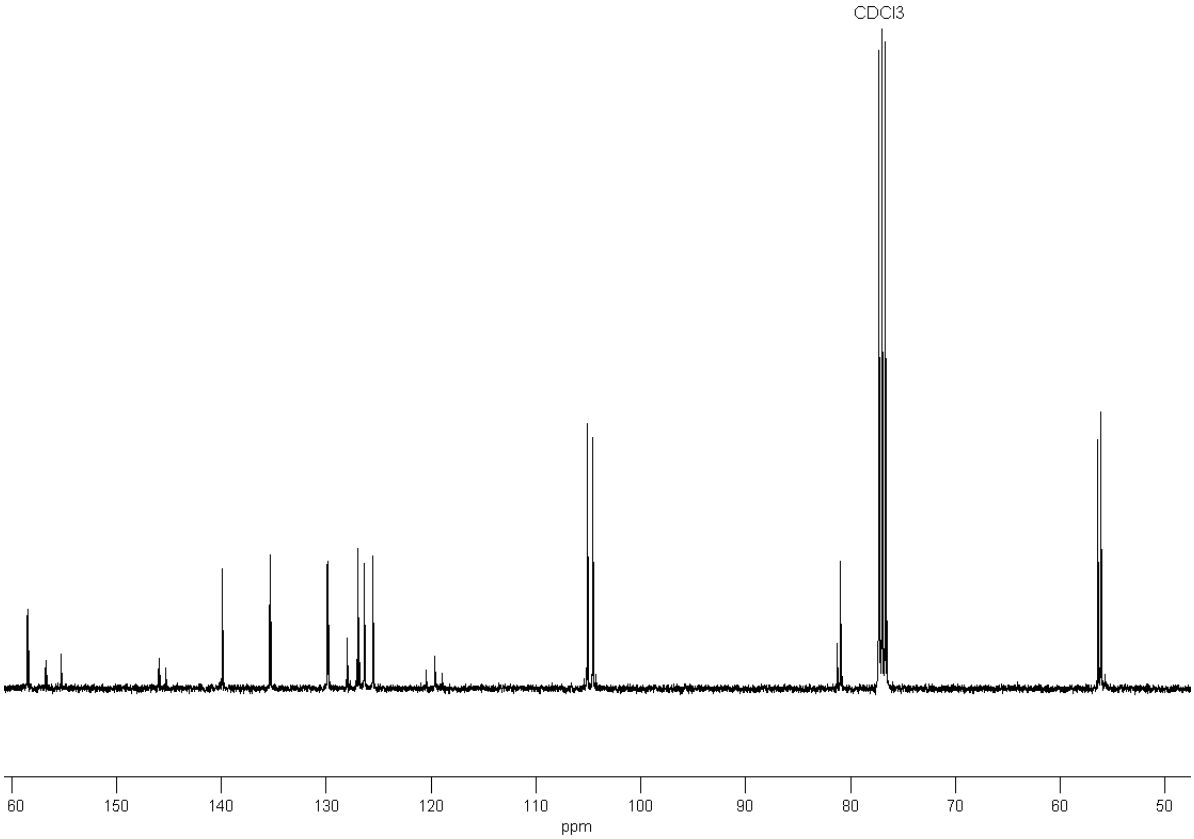

Figure S6. ^{13}C NMR spectrum (100 MHz, $CDCl_3$, 298 K) of 2,9-bis-(2,6-dimethoxyphenyl)-3-ethynyl-[1,10]-phenanthroline (**11**).

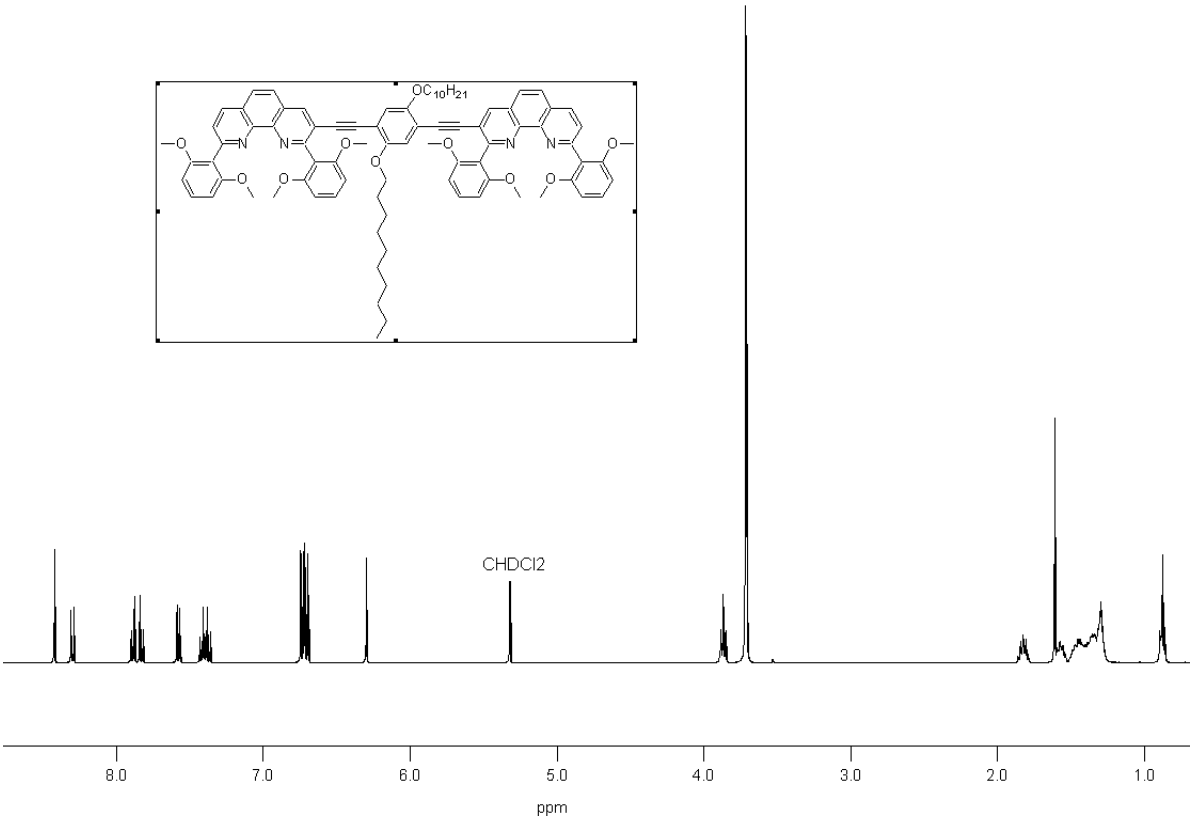

Figure S7. ^{1}H NMR spectrum of **6** (400 MHz, CD_2Cl_2, 298 K).

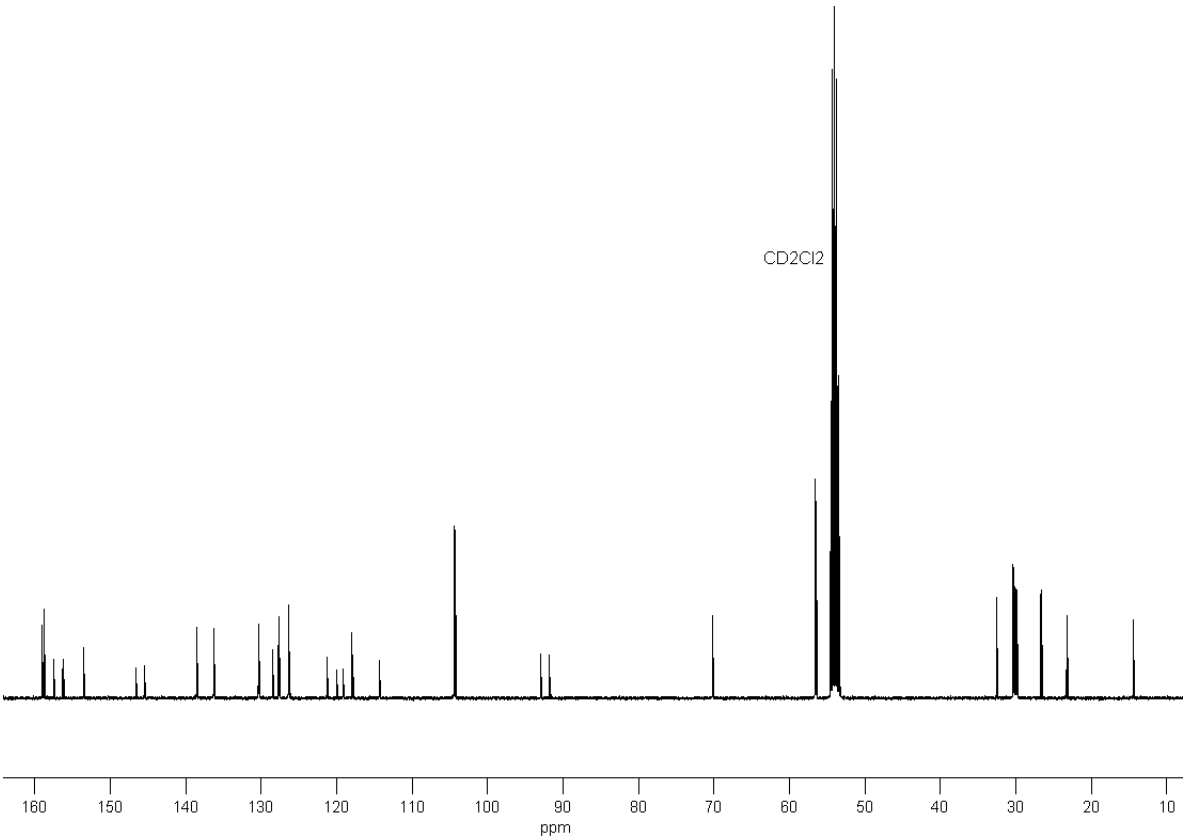

Figure S8. ^{13}C NMR spectrum of **6** (100 MHz, CD_2Cl_2, 298 K).

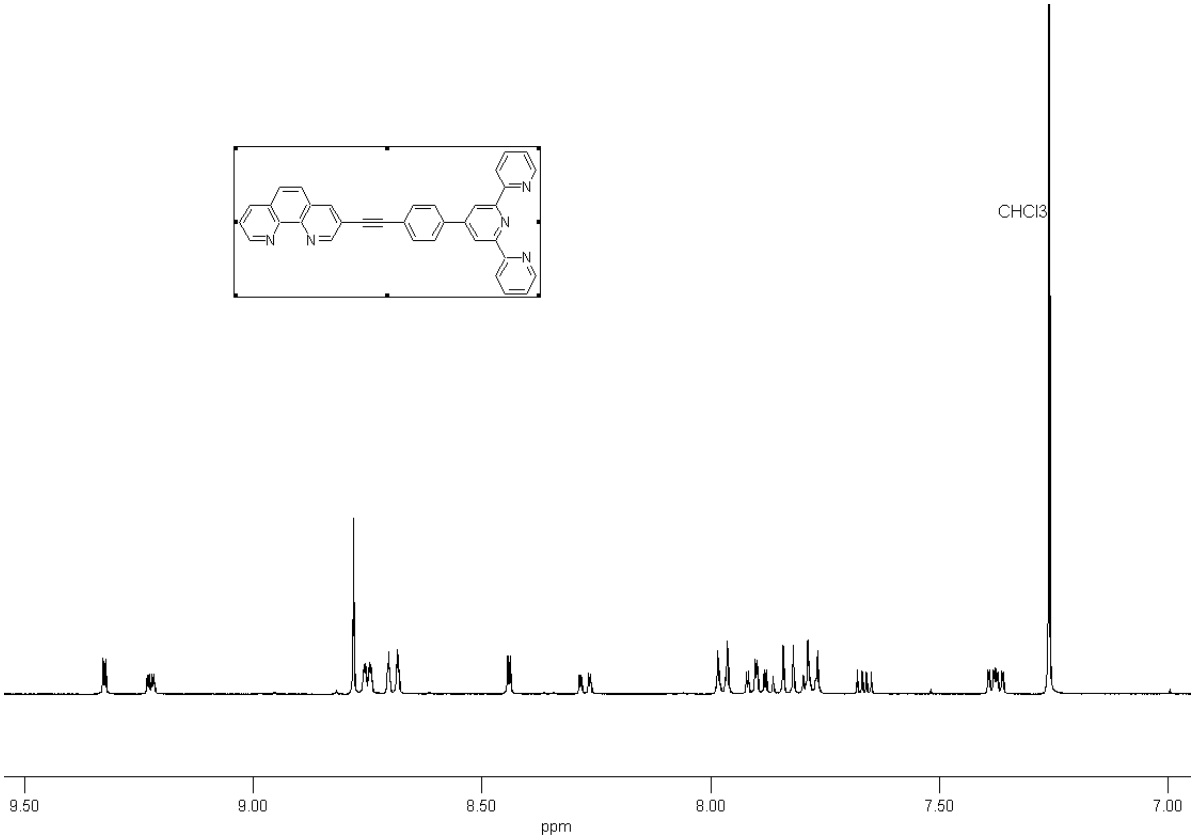

Figure S9. ^{1}H NMR spectrum of **7** (400 MHz, $CDCl_3$, 298 K).

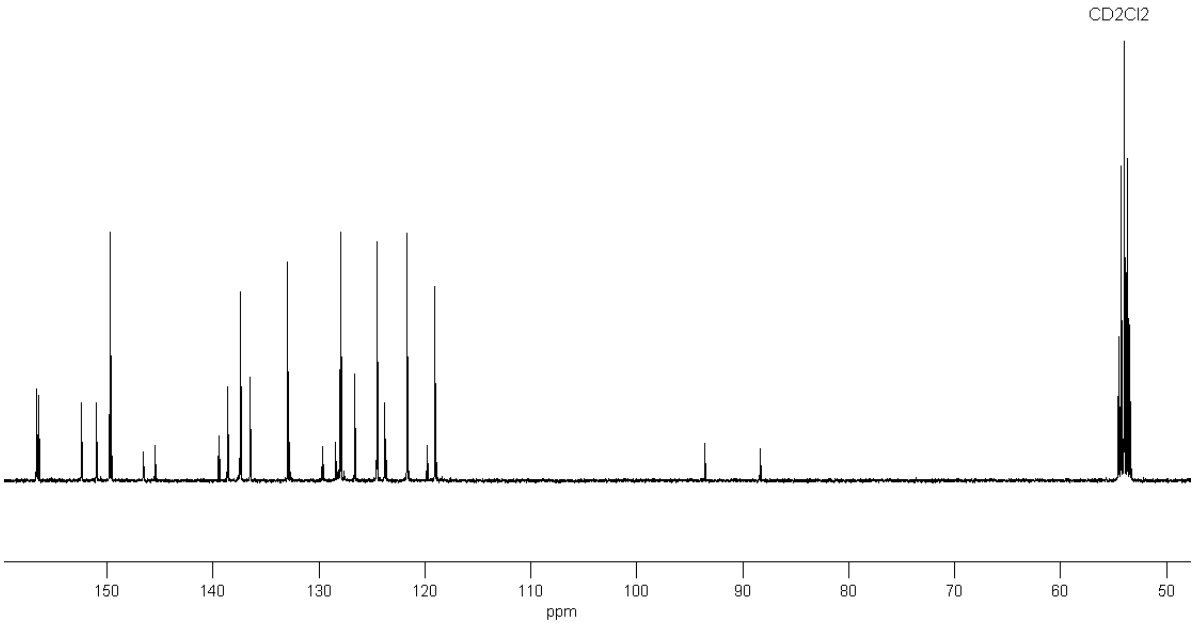

Figure S10. ^{13}C NMR spectrum of **7** (100 MHz, CD_2Cl_2, 298 K).

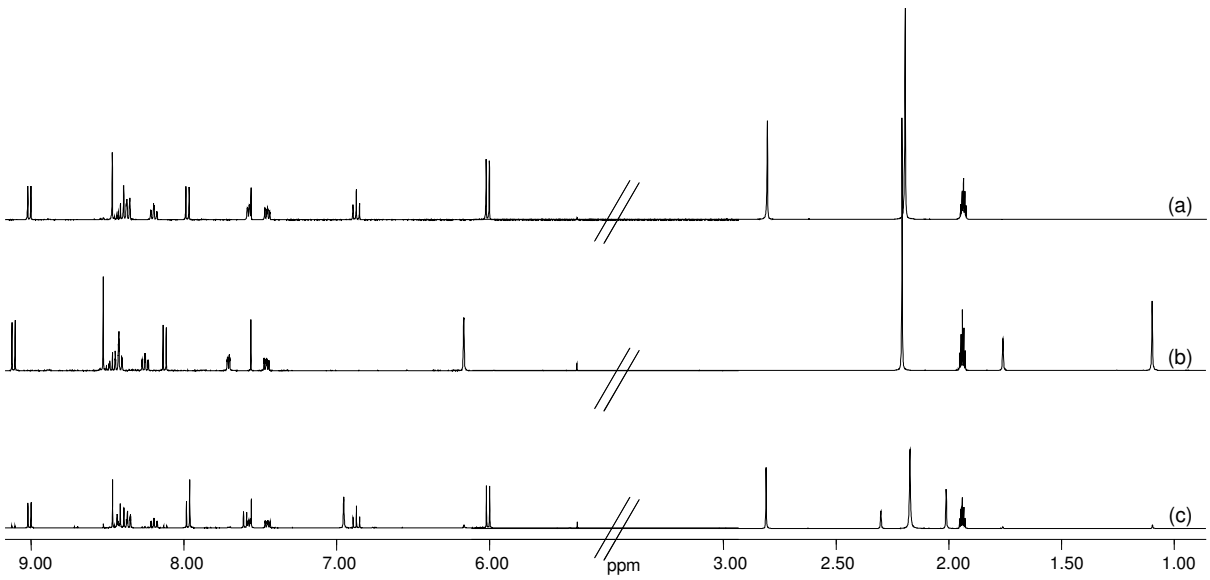

Figure S11. ^{1}H NMR (400 MHz, 298 K, $CD_3CN/CDCl_3$ v/v 3:1) spectra of (a) [Zn(**2**)(**3**)](OTf)$_2$, (b) [Zn(**1**)(**3**)](OTf)$_2$ and (c) an equimolar mixture of **1**,**2**,**3** in presence of Zn(OTf)$_2$.

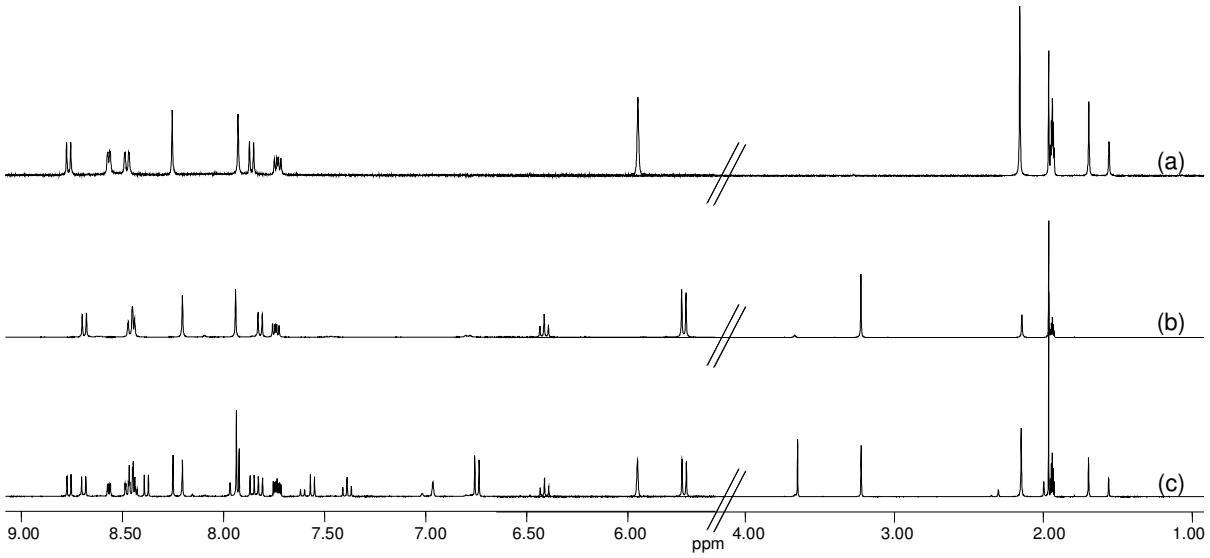

Figure S12. ^{1}H NMR (400 MHz, 298 K, CD_3CN) spectra of (a) [Cu(**1**)(**4**)](PF$_6$), (b) [Cu(**2**)(**4**)](PF$_6$) and (c) an equimolar mixture of **1**,**2**,**4** in presence [Cu(MeCN)$_4$](PF$_6$).

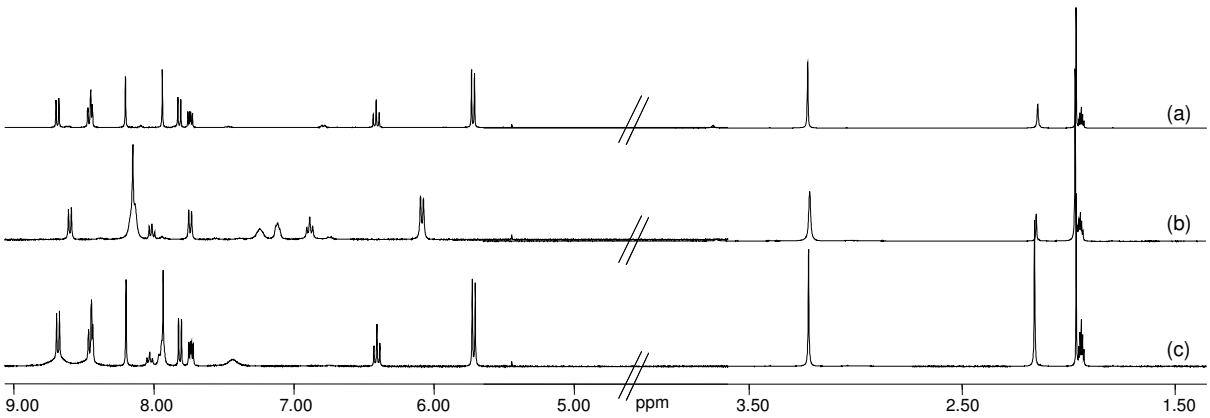

Figure S13. ^{1}H NMR (400 MHz, 298 K, CD_3CN) spectra of (a) [Cu(**2**)(**4**)](PF_6), (b) [Cu(**2**)(**3**)](PF_6) and (c) an equimolar mixture of **2**,**3**,**4** in presence of [Cu(MeCN)$_4$](PF_6).

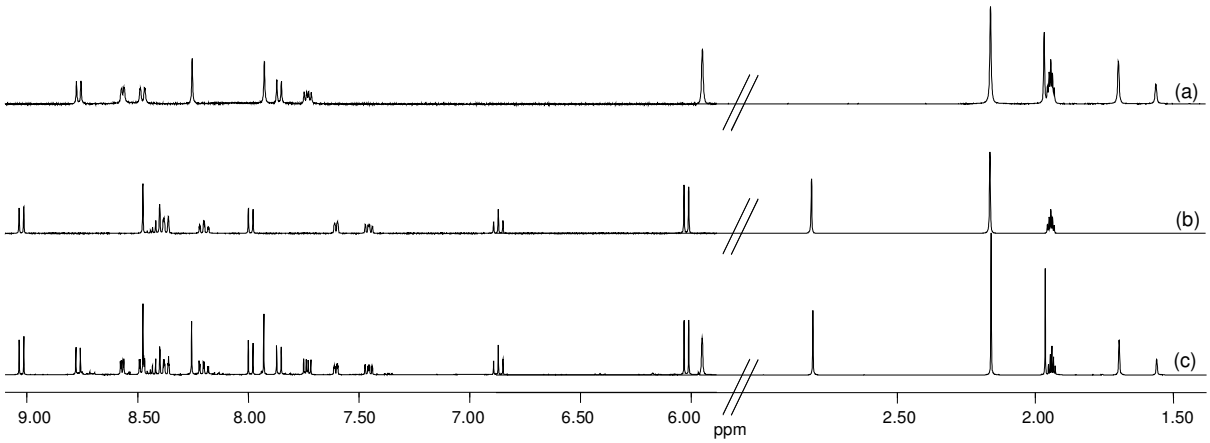

Figure S14. ^{1}H NMR (400 MHz, 298 K, CD_3CN) spectra of (a) [Cu(**1**)(**4**)](PF_6), (b) [Zn(**2**)(**3**)]($OTf)_2$ and (c) an equimolar mixture of **1**,**2**,**3**,**4** in presence of $Zn(OTf)_2$ and [Cu(MeCN)$_4$](PF_6).

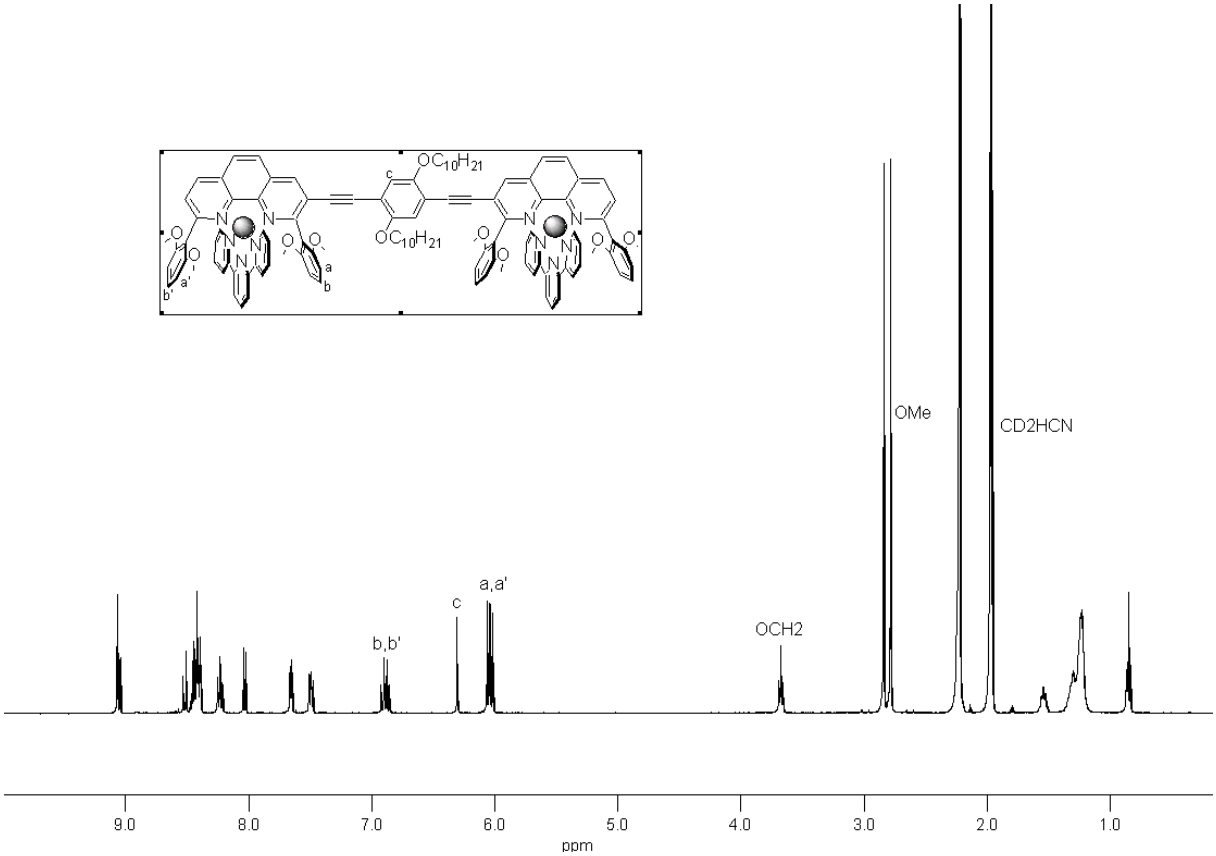

Figure S15. ^{1}H NMR spectrum of the rack assembly $[Zn_2(\mathbf{6})(\mathbf{3})_2](OTf)_4$ (400 MHz, CD_3CN, 298 K).

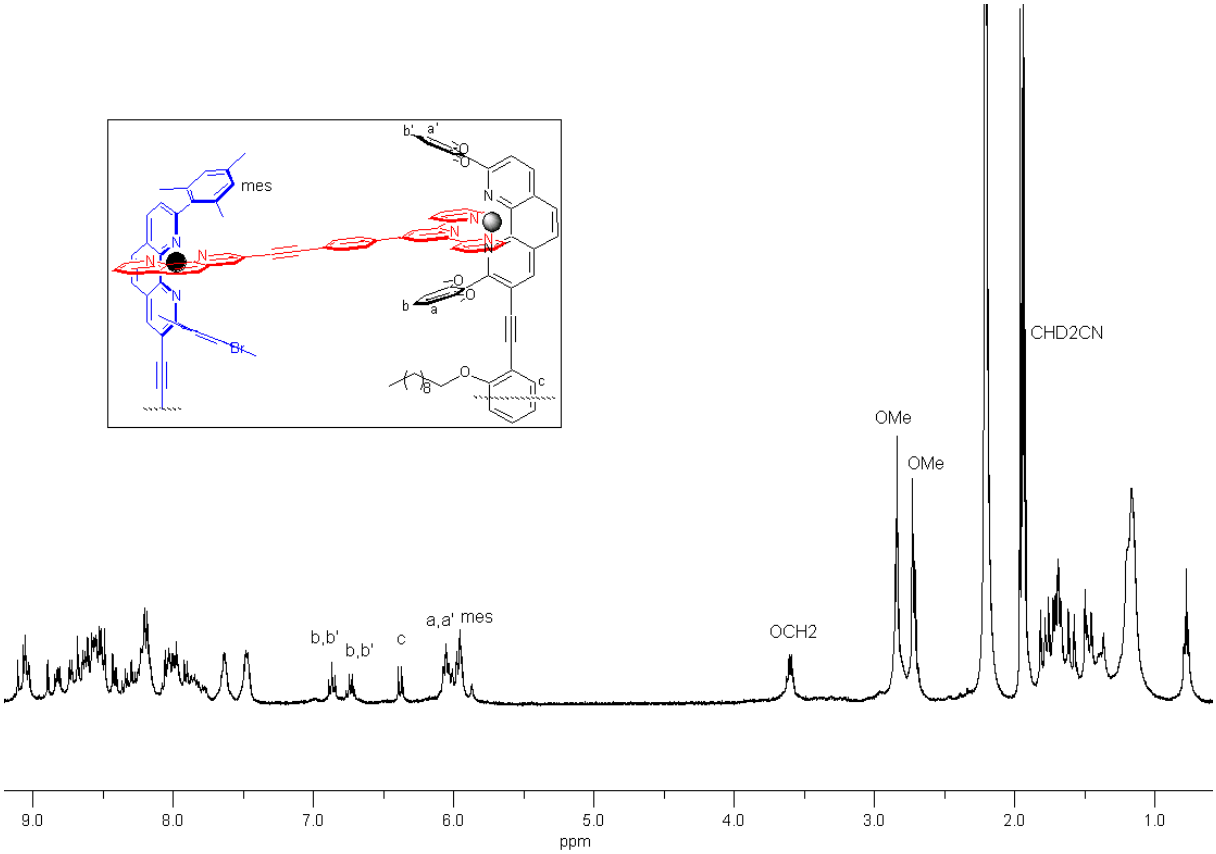

Figure S16. ^{1}H NMR spectrum of the trapezoid **T** (400 MHz, CD_3CN, 298 K).

ESI-MS spectra

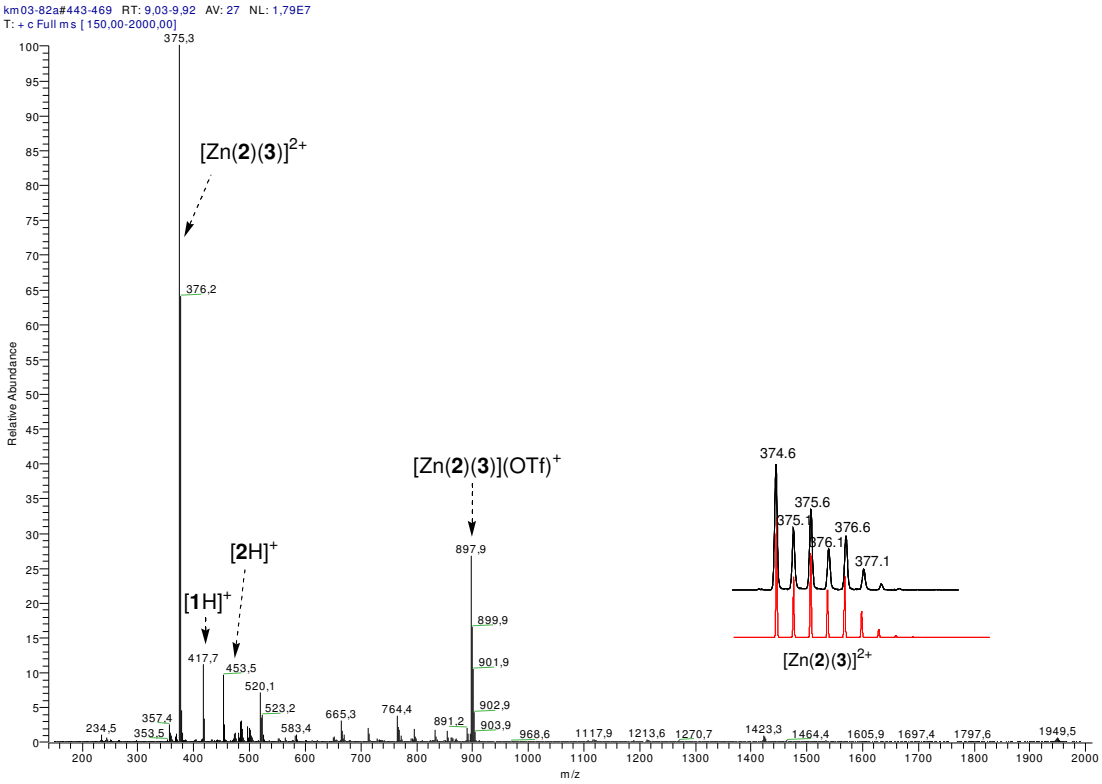

Figure S17. ESI-MS spectrum of an equimolar mixture of **1**,**2**,**3** and $Zn(OTf)_2$ in acetonitrile/chloroform (v/v 3:1). The spectrum recorded after stirring all components at 60 °C for 2 h.

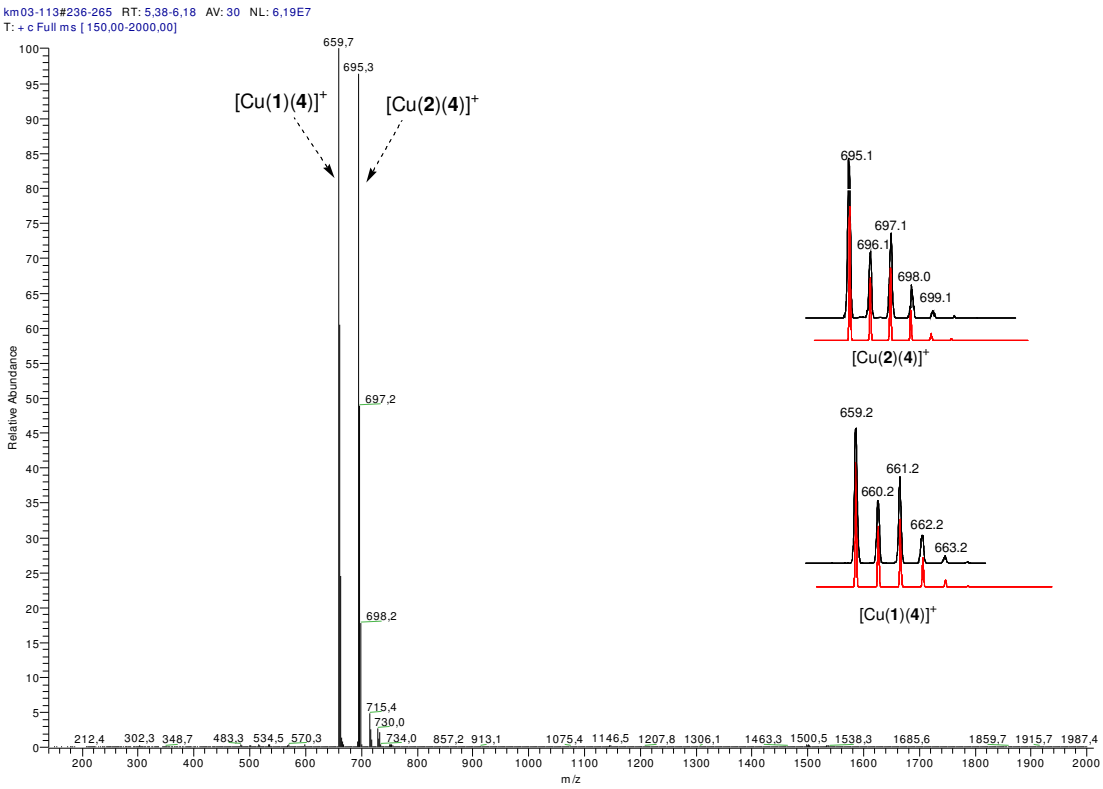

Figure S18. ESI-MS spectrum of an equimolar mixture of **1**,**2**,**4** and $[Cu(MeCN)_4](PF_6)$ in acetonitrile. The spectrum recorded after refluxing all components in acetonitrile for 2 h.

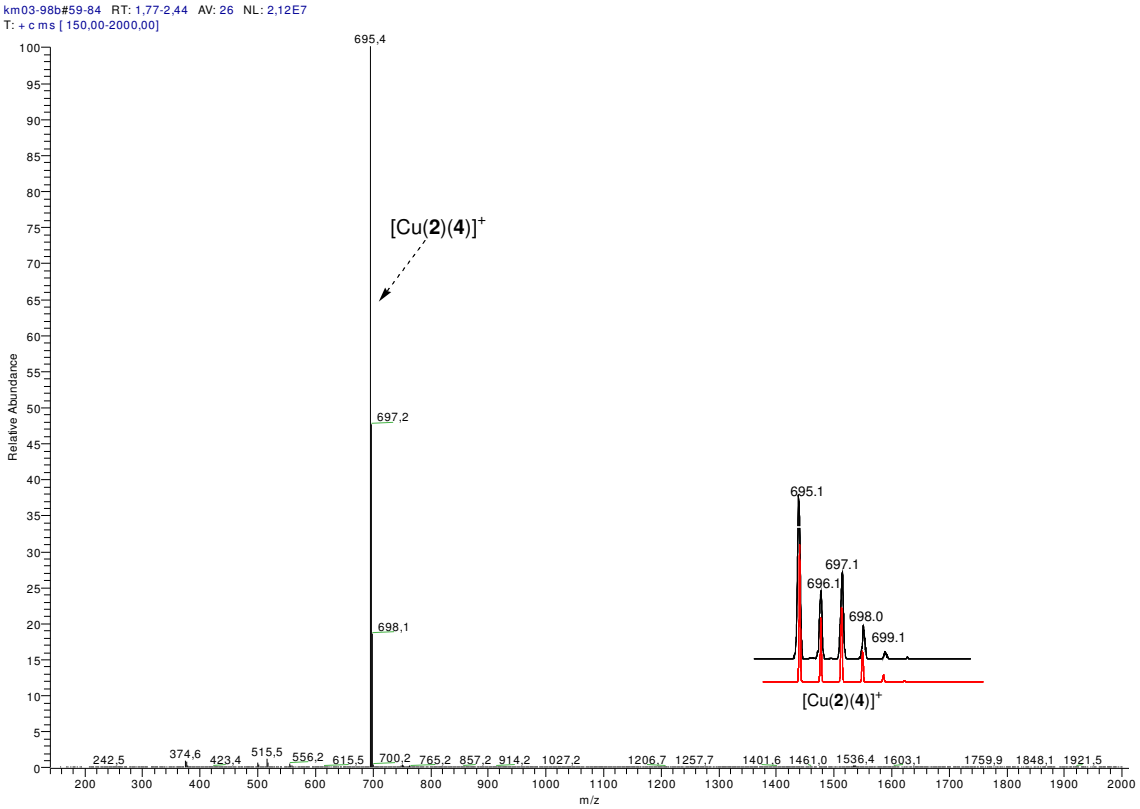

Figure S19. ESI-MS spectrum of an equimolar mixture of **2**,**3**,**4** and $[Cu(MeCN)_4](PF_6)$ in acetonitrile. The spectrum recorded after refluxing all components in acetonitrile for 2 h.

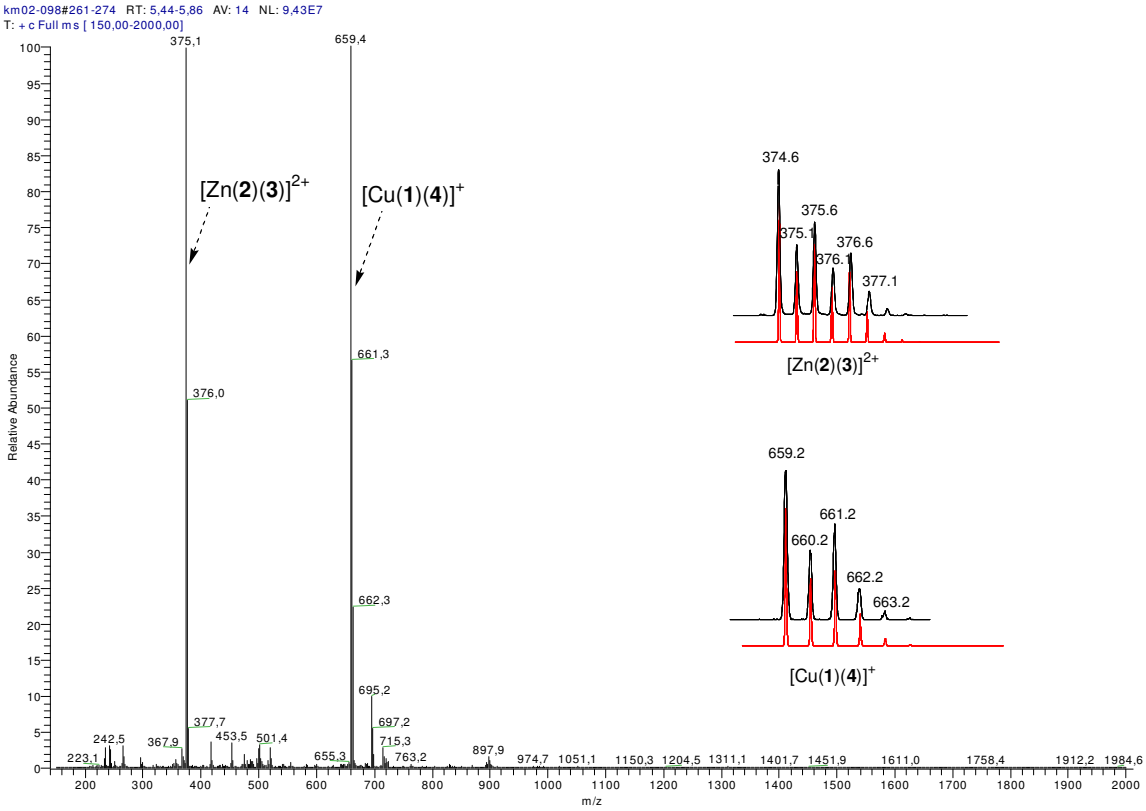

Figure S20. ESI-MS spectrum of an equimolar mixture of **1**,**2**,**3**,**4** in presence of $Zn(OTf)_2$ and $[Cu(MeCN)_4](PF_6)$ in acetonitrile. The spectrum recorded after refluxing all components in acetonitrile for 2 h.

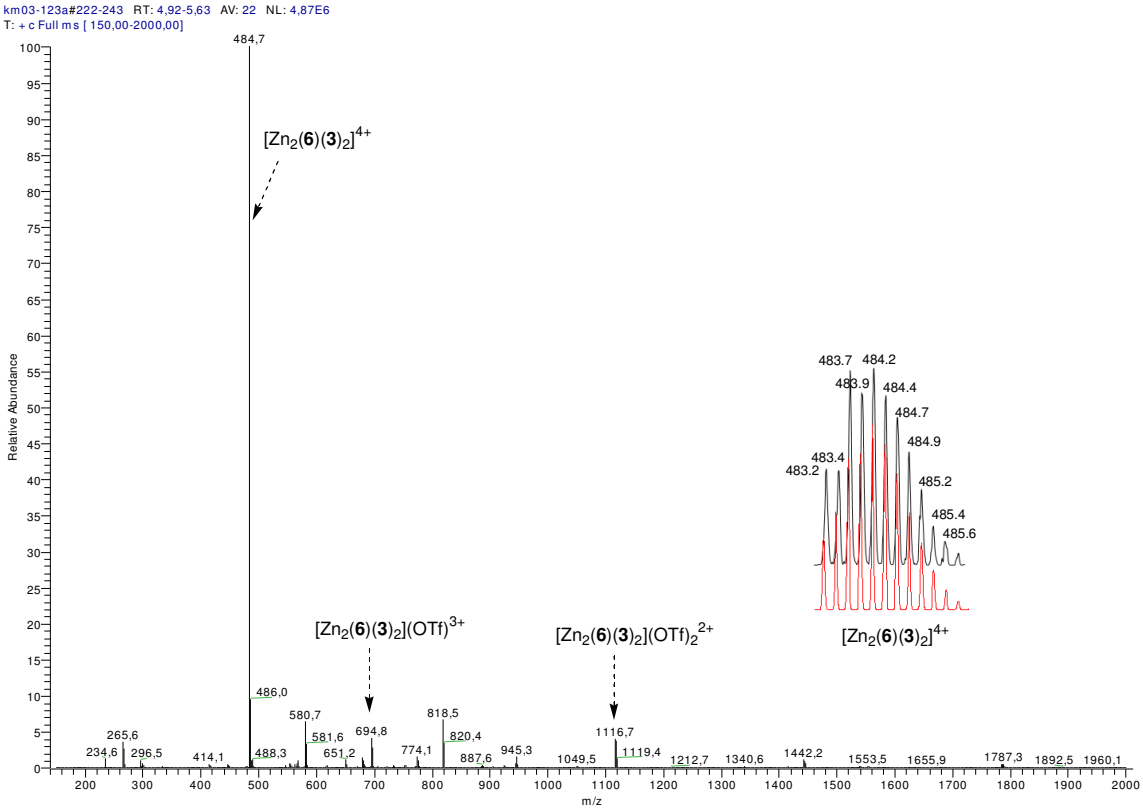

Figure S21. ESI-MS spectrum of rack assembly $[Zn_2(\mathbf{6})(\mathbf{3})_2](OTf)_4$ (in acetonitrile) and experimental isotopic distributions (black lines) along with calculated isotopic distributions (red lines) for the four charged species.

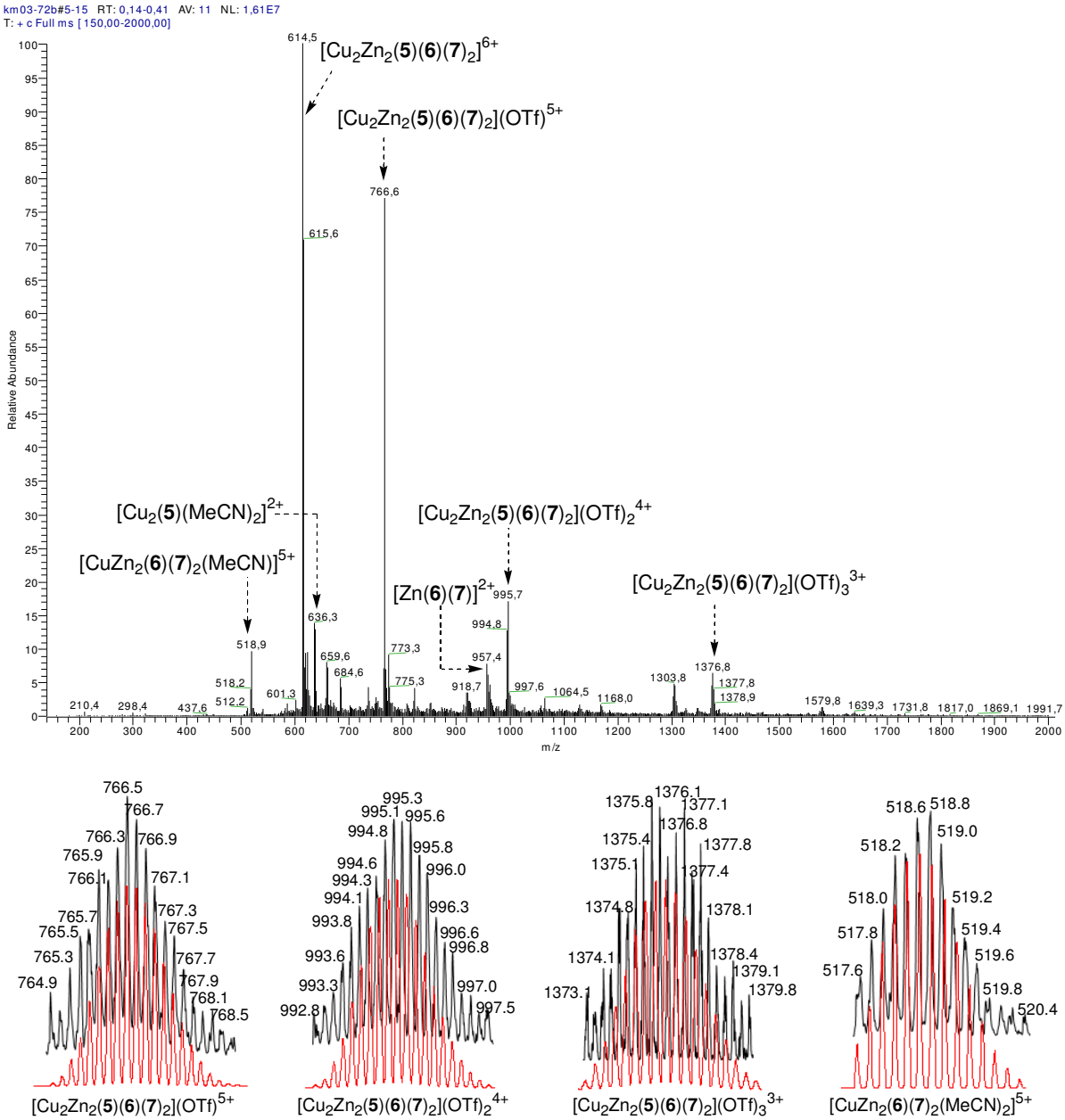

Figure S22. ESI-MS spectrum of **T** = $[Cu_2Zn_2(\mathbf{5})(\mathbf{6})(\mathbf{7})_2](OTf)_4(PF_6)_2$ (in acetonitrile) and experimental isotopic distributions (black lines) along with calculated isotopic distributions (red lines) for the different charged species obtained after the loss of counter anion(s).

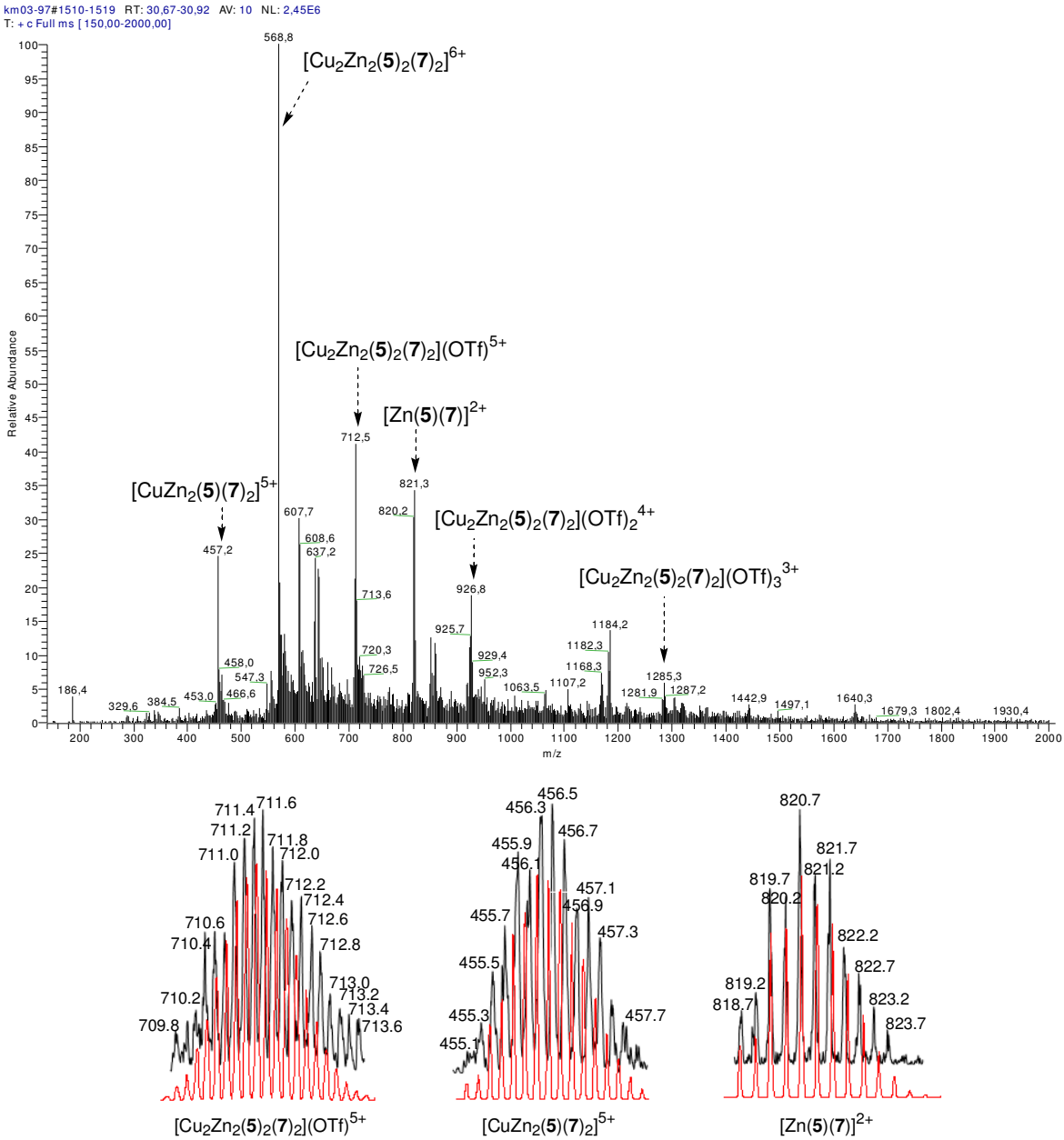

Figure S23. ESI-MS spectrum of $\mathbf{R_S}$ = $[Cu_2Zn_2(\mathbf{5})_2(\mathbf{7})_2](OTf)_4(PF_6)_2$ (in acetonitrile) and experimental isotopic distributions (black lines) along with calculated isotopic distributions (red lines) for the different charged species obtained after the loss of counter anion(s).

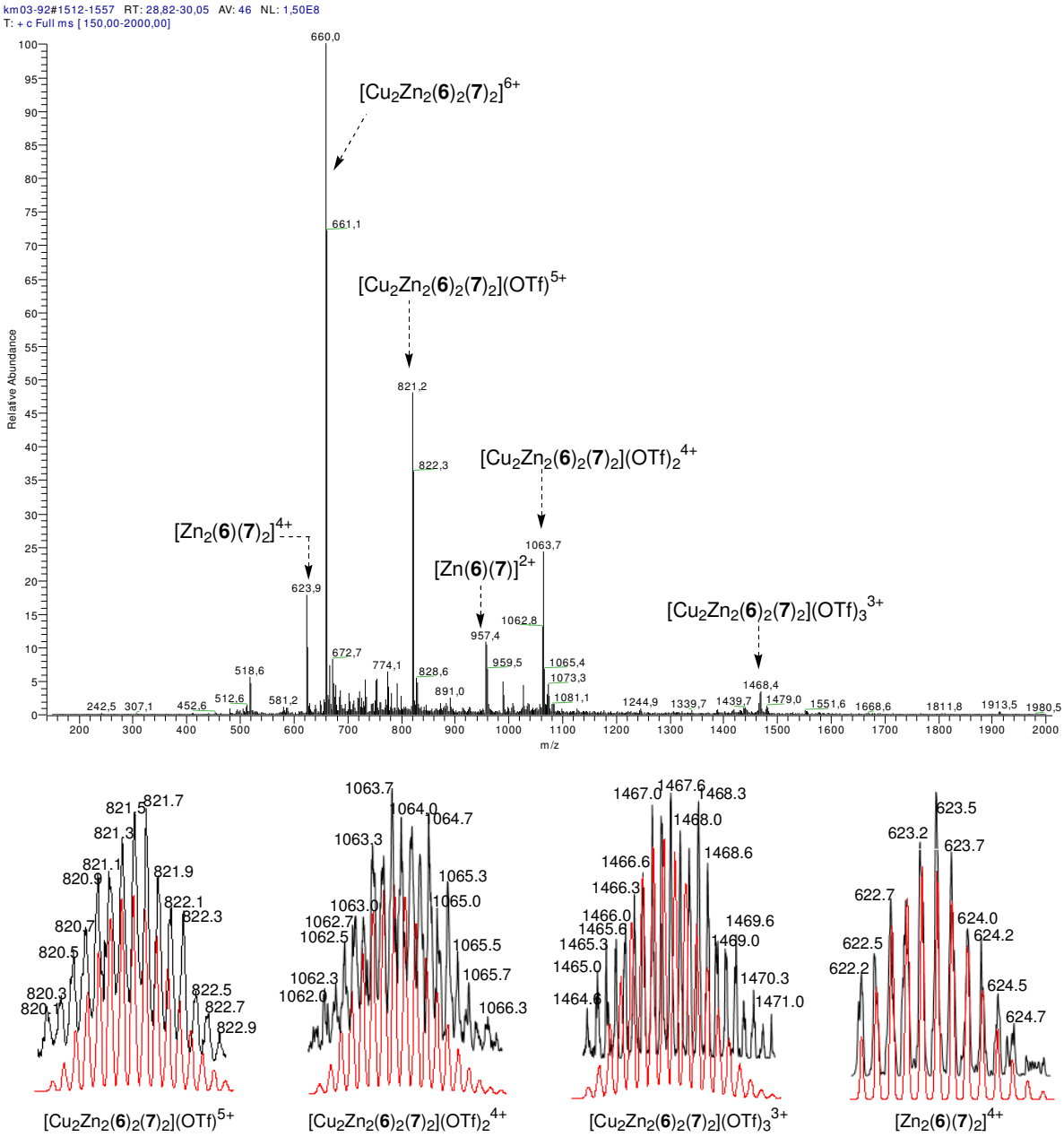

Figure S24. ESI-MS spectrum of $\mathbf{R_L}$ = $[Cu_2Zn_2(\mathbf{6})_2(\mathbf{7})_2](OTf)_4(PF_6)_2$ (in acetonitrile) and experimental isotopic distributions (black lines) along with calculated isotopic distributions (red lines) for the different charged species obtained after the loss of counter anion(s).

Differential Pulse Voltammgrams

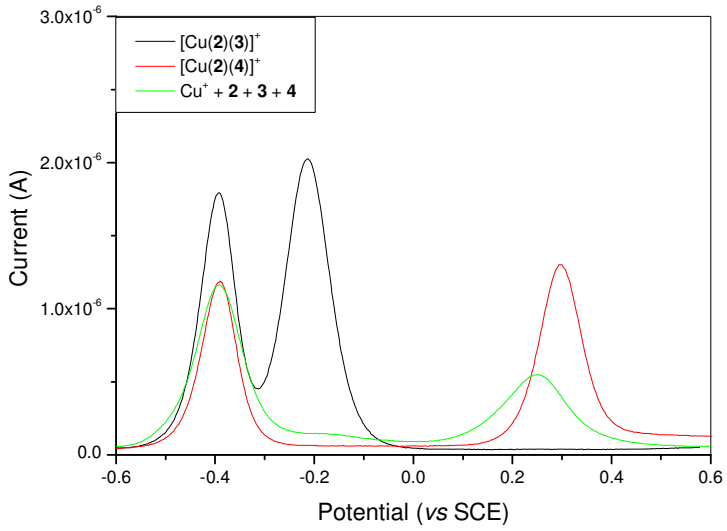

Figure S25. Differential pulse voltammetry (DPV) investigation of [Cu(**2**)(**3**)](PF_6) (black), [Cu(**2**)(**4**)](PF_6) (red) and an equimolar mixture of mixture **2**,**3**,**4** in presence of [Cu(MeCN)$_4$](PF_6) (green). The experiments were carried out in dry acetonitrile with 0.1 M nBu$_4$NPF$_6$ as electrolyte against a Ag wire as a quasi-reference electrode and 2,4,6-triphenylpyrylium tetrafluoroborate as internal standard (scan rate of 20 mVs^{-1} and a pulse height of 2 mV).

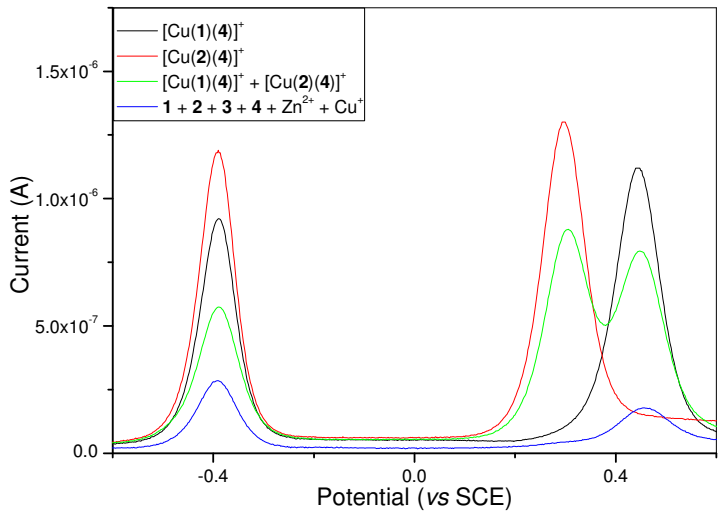

Figure S26. Differential pulse voltammetry (DPV) investigation of [Cu(**1**)(**4**)](PF_6) (black), [Cu(**2**)(**4**)](PF_6) (red), mixture of [Cu(**1**)(**4**)](PF_6) and [Cu(**2**)(**4**)](PF_6) (green), and an equimolar mixture of **1**,**2**,**3**,**4** in presence of [Cu(MeCN)$_4$](PF_6) and Zn(OTf)$_2$ (blue). The experiments were carried out in dry acetonitrile with 0.1 M nBu$_4$NPF$_6$ as electrolyte against a Ag wire as a quasi-reference electrode and 2,4,6-triphenylpyrylium tetrafluoroborate as internal standard (scan rate of 20 mVs^{-1} and a pulse height of 2 mV).

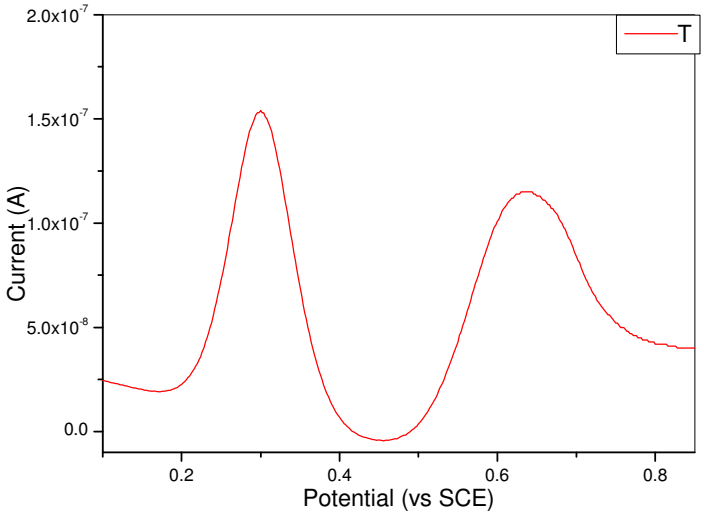

Figure S27. Differential pulse voltammetry (DPV) investigation of trapezoid **T** = $[Cu_2Zn_2(\mathbf{5})(\mathbf{6})(\mathbf{7})_2](OTf)_4(PF_6)_2$. The experiment was carried out in dry acetonitrile with 0.1 M nBu$_4$NPF$_6$ as electrolyte against a Ag wire as a quasi-reference electrode and 1,1'-dimethyl ferrocene as internal standard (scan rate of 20 mVs^{-1} and a pulse height of 2 mV).

Deconvolution of the DPV

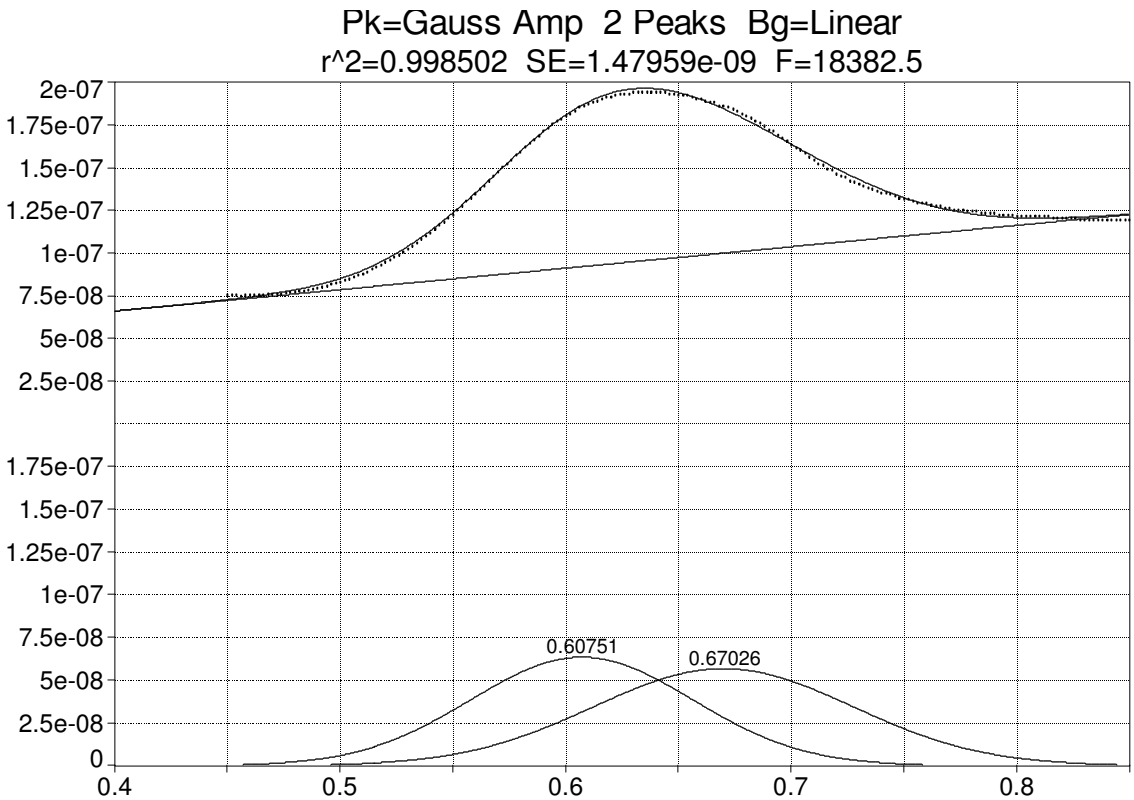

Figure S28. Deconvoluted differential pulse voltammgram of trapezoid **T** = $[Cu_2Zn_2(\mathbf{5})(\mathbf{6})(\mathbf{7})_2](OTf)_4(PF_6)_2$.

Fitted Parameters

r^2 Coef Det	DF Adj r^2	Fit Std Err	F-value
0.99850237	0.99843997	1.4796e-09	18382.5228

Peak	Type	a0	a1	a2
1	Gauss Amp	6.3375e-08	0.60750808	0.04923810
2	Gauss Amp	5.6618e-08	0.67026210	0.05760980
B	Linear Bg	1.5649e-08	1.2574e-07	

Measured Values

Peak	Type	Amplitude	Center	FWHM	Asym50	FW Base	Asym10
1	Gauss Amp	6.3375e-08	0.60750808	0.11594686	1.00000000	0.23209178	1.00000000
2	Gauss Amp	5.6618e-08	0.67026210	0.13566071	1.00000000	0.27155315	1.00000000

Peak	Type	Anlytc Area	% Area	Int Area	% Area	Centroid	Moment2
1	Gauss Amp	7.8218e-09	48.8930294	7.8164e-09	48.9000358	0.60762586	0.00240578
2	Gauss Amp	8.176e-09	51.1069706	8.1681e-09	51.0999642	0.67010043	0.00328364
	Total	1.5998e-08	100.000000	1.5985e-08	100.000000		

Parameter Statistics

Peak 1 Gauss Amp

Parm	Value	Std Error	t-value	95	
Amp	6.3375e-08	3.3672e-08	1.88215188	-3.036e-09	1.2979e-07
Ctr	0.60750808	0.00940378	64.6025446	0.58896071	0.62605546
Wid	0.04923810	0.00294342	16.7281787	0.04343269	0.05504350

Peak 2 Gauss Amp

Parm	Value	Std Error	t-value	95	
Amp	5.6618e-08	2.4678e-08	2.29429848	7.9454e-09	1.0529e-07
Ctr	0.67026210	0.02549894	26.2858813	0.61996973	0.72055446
Wid	0.05760980	0.00775553	7.42822471	0.04231333	0.07290627

Baseline Linear Bg

Parm	Value	Std Error	t-value	95	
a0	1.5649e-08	1.2155e-09	12.8748277	1.3252e-08	1.8046e-08
a1	1.2574e-07	1.9353e-09	64.9721191	1.2192e-07	1.2956e-07

Analysis of Variance

r^2 Coef Det	DF Adj r^2	Fit Std Err
0.99850237	0.99843997	1.4796e-09

Source	Sum of Squares	DF	Mean Square	F
Regr	2.8169942e-13	7	4.0242775e-14	18382.523
Error	4.2251303e-16	193	2.1891867e-18	
Total	2.8212194e-13	200		

Details of Fit

Set Convergence	State	Iterations	Minimization	Extent
1E-6	Converged	106	Least Squares	1/1

Curvature Matrix	Constraints	Violated
Sparse-Roots	25.0000-5.00000-50.0000- None - None	0